Explanation of the dissipation observed in several high-temperature superconductors using a modified Ambegaokar-Halperin model

R. J. Soulen, Jr., T. L. Francavilla, W. W. Fuller-Mora, and M. M. Miller
Naval Research Laboratory, Washington, D.C. 20375-5000

C. H. Joshi, W. L. Carter, A. J. Rodenbush, M. D. Manlief, and D. Aized
American Superconductor Corporation, Westborough, Massachusetts 01581
(Received 7 December 1993; revised manuscript received 14 March 1994)

We have measured the current-voltage (I-V) characteristics of several high-temperature-superconducting materials with widely different morphologies (bulk Ag/Pb-Bi-Sr-Ca-Cu-O tapes, thin films of Y-Ba-Cu-O, and melt-textured, bulk Y-Ba-Cu-O samples). The I-V curves were taken at several magnetic fields ranging from 0 to 8 T. The measurements were carried out at three temperatures (4.2, 27, and 77 K) where the samples were immersed in liquid cryogens to ensure good thermal equilibrium. We compared our experimental results to the predictions of dissipation in superconductors made by the following physical models: modified Ambegaokar-Halperin, flux creep, vortex glass, collective flux creep, and a power law. The fits were extremely good for the first model and were not nearly as good for the others. Using the modified Ambegaokar-Halperin model, the critical current I_c, the normal-state resistance R_n, and γ, which is proportional to the pinning potential $U(H,T)$, were obtained for each material. Since the Ambegaokar-Halperin model is the only one which uniquely defines I_c, we conclude that its use puts this parameter on a solid physical basis.

I. INTRODUCTION

The effect of magnetic field on the transport properties of high-T_c superconductors, in particular the resistance $R(H,T)$ and the nonlinear current-voltage (I-V) characteristics, has received considerable experimental and theoretical attention over the past few years. The preponderance of these results, however, has not led to a consensus as to the proper explanation of the observed dissipation. In fact, the results are generally inconsistent.

For instance, Palstra *et al.*[1] studied the resistance of single crystals of $YBa_2Cu_3O_7$ (YBCO) and $Bi_{2.2}Sr_2Ca_{0.8}Cu_2O_8$ (BSCCO) and interpreted their results in terms of a thermally activated flux-flow (TAFF) model which is based on the original work of Anderson and Kim.[2] On the other hand, Koch *et al.*[3] studied the resistance and I-V curves of oriented thin films of YBCO and interpreted their results in terms of a vortex-glass (VG) model.[4] An alternative explanation of the Koch results was advanced in a comment by Coppersmith, Inui, and Littlewood,[5] who fitted the data with the Ambegaokar-Halperin (AH) model.[6] This interpretation was rebutted by Koch *et al.* in favor of the VG model.[7] Polycrystalline samples of high-temperature superconductors have been studied as well: Wright, Zhang, and Erbil[8] measured the resistance and I-V curves near the superconducting transition temperature T_c of granular $Bi_{1.7}Pb_{0.2}Sb_{0.1}Sr_2Ca_2Cu_3O_{10}$ and used the AH model to determine pinning energies and T_c. Granular YBCO was treated using the same model by Gaffney, Peterson, and Bednar.[9] Conversely, Miu *et al.*[10] studied granular YBCO and $Bi_2Sr_2Ca_2Cu_3O_{10}$ samples and fitted the results most successfully to a collective flux-creep (CFC) model.[11,12]

The purpose of this paper is to present the results of an extensive study of the I-V curves of samples with three very different morphologies [oriented thin films of YBCO, melt-textured YBCO, and bulk composite $Ag/Bi_{1.8}Pb_{0.3}Sr_{1.9}Ca_2Cu_{3.1}O_{10}$ (Ag/PBSCCO) wires]. The current and voltage were varied over as large a range as possible and with a high density of points. Measurements were made at three temperatures where the samples could be immersed in a liquid cryogen to assure isothermal conditions. The I-V curves were also measured at several magnetic fields to provide a dense spacing of fitting parameters in order to define their functional dependence on this variable.

The I-V curves were fitted by the predictions of the four models introduced above (TAFF, VG, AH, CFC), as well as to a polynomial form often introduced on an empirical basis[13] in order to define I_c. Although over some of the range of magnetic field or temperature, one or more of the models fit the data reasonably well, we found that only the AH model consistently fit all the data well over the entire range of measured values.

II. THE AMBEGAOKAR-HALPERIN MODEL AND ITS APPLICATION TO DISSIPATION IN SUPERCONDUCTORS IN A MAGNETIC FIELD

Before presenting the modified Ambegaokar-Halperin model we make a distinction concerning current flow in the materials under study. The samples we have studied can be divided into two categories: *composite materials* consisting of a bulk superconductor imbedded in a normal-metal matrix, and *homogeneous materials* consisting simply of a superconductor. In homogeneous materials the current is carried by the superconductor and the

0163-1829/94/50(1)/478(10)/$06.00

theory may be applied directly. In the composites, however, "current sharing" occurs; that is, the total applied current I divides into two parallel components, I_s and I_n. The former represents the current flowing through the superconductor, while the latter represents the current flowing through the normal-metal regions. Thus, in the case of the composite material,

$$I = I_s + I_n = I_s + G_n V , \tag{1}$$

where G_n is the conductance of the normal-metal path and V is the voltage drop. Where the distinction between I and I_s is relevant, it is understood that the AH model refers only to I_s.

Ambegaokar and Halperin[6] derived the differential equation for a circuit containing a single Josephson junction. Taking into account the effect of thermal noise, they solved that equation to obtain $V(I_s)$ as a function of the noise-rounding parameter, $\gamma \equiv E_J/k_B T = \phi_o I_c/2\pi k_B T$. Here k_B is Boltzmann's constant, ϕ_o is the flux quantum, I_c is the critical current of the junction in the absence of thermal fluctuations, and E_J is the Josephson coupling energy. Their general solution to the differential equation is written as an integral:

$$V = (I_c R_J)\frac{4\pi}{\gamma}\left\{ (e^{\pi\gamma x}-1)^{-1}\left[\int_0^{2\pi} d\theta f(\theta)\right]\left[\int_0^{2\pi} d\theta' \frac{1}{f(\theta')}\right] + \int_0^{2\pi} d\theta \int_\theta^{2\pi} d\theta' \frac{f(\theta)}{f(\theta')}\right\}^{-1} , \tag{2}$$

where R_J is the normal resistance of the junction, $f(\theta) = \exp[-U(\theta)/k_B T]$, and $x = (I_s/I_c)$.

When γ is large and when $x < 1$, AH found a closed-form solution for $V(I_s)$

$$V = (2I_c R_J)(1-x^2)^{1/2}\exp[-\gamma F(x)]\sinh\left[\frac{\pi\gamma x}{2}\right] , \tag{3}$$

where $F(x) = (1-x^2)^{1/2} + x\sin^{-1}x$. Using two additional approximations $\ln(1-x^2) \sim 0$ and $\sinh(\pi\gamma x/2) \sim 0.5\exp(\pi\gamma x/2)$, which are consistent with the above conditions on γ and x, an even simpler equation can be written,

$$I_s = k_1 + k_2 \ln V , \tag{4}$$

where

$$k_1 = [I_c(2/\pi) - (2I_c/\pi\gamma)\ln(I_c R_J)]$$

and $k_2 = (2I_c/\pi\gamma)$. For the composite materials we found that it was very convenient to use the analytic form, Eq. (1) with I_s defined by Eq. (4), to fit the I-V curves to obtain approximate values of R_n, γ, and I_c which were then used as starting values in the more accurate fits[14] employing the more cumbersome numerical integration prescribed by Eq. (2).

The differential resistance $R_d \equiv dV/dI$ will be needed later in this paper; from Eqs. (1) and (4) we derive a convenient analytic expression for this quantity:

$$R_d = \frac{G_n}{[1 + (k_2/VG_n)]} . \tag{5}$$

We argue that the voltage drop in a superconductor in the presence of a magnetic field is given by the AH solutions provided that a single parameter γ is redefined. In the same paper in which the I-V curve was derived, AH showed that the differential equation for the Josephson junction was equivalent to the solution of the problem of viscous Brownian motion of a particle subject to a particular potential U given by the expression

$$U = -\frac{hI_c}{4\pi e}(x\theta + \cos\theta) = -E_J(x\theta + \cos\theta) . \tag{6}$$

A periodic potential of the same form as that given by Eq. (6) could, however, also be a good representation of the pinning sites distributed throughout a bulk superconductor. Alternatively, Tinkham and Lobb have argued that a continuous superconductor sullied by a sprinkling of localized defects can be considered as mathematically equivalent to a granular array of Josephson junctions for which the AH model has been shown to apply.[15] For either circumstance then the AH model may be applied to the dissipation manifested in the I-V curves of current-carrying superconductors when exposed to a magnetic field. Tinkham,[16] in fact, used the AH expression for the slope of the I-V curve at $V = 0$ in this case to describe the temperature and magnetic-field dependence of the resistance of YBCO. One of the present authors (RJS),[17] has suggested that this approach could be extended equally well to calculate the whole I-V characteristic. Indeed, all that is needed to adapt the I-V solutions given by AH to the present situation is to replace the Josephson coupling energy, E_J, appearing in the definition of γ by a pinning potential $U(H,T)$.

It is very important to emphasize, however, that the critical current defined by the AH model is quite different than that generally defined to account for the effects of dissipation induced, for example, in superconducting magnet wires. To emphasize the distinction, we designate the former as I_c^{AH} and the latter as I_c^{VC}. Within the framework of the AH model, I_c^{AH} refers roughly to the point on the I-V curve where the superconductivity has vanished (roughly, where $I = V/R_J$ at large voltages). Alternatively, the product $V_c = I_c^{\mathrm{AH}} R_J$ represents the voltage at which the Josephson junction (flux line) has sufficient energy to freely skip across the peaks of the periodic potential (the flux-flow limit). In the case of dissipation in magnets, however, I_c^{VC} refers to the current at which dissipation just begins to be observable, that is, when V exceeds a particular, small value V_o. Thus the critical current is defined by a "voltage criterion" or, more precisely, it is expressed in terms of a particular value of the electric field E (typically, 1 μV/cm). It is clear from these definitions that I_c^{AH} is larger than I_c^{VC}. The former definition has the advantage that it is uniquely defined by the AH model and related physical principles rather than by a convention. The exact converse obtains for the latter. Throughout the remainder of this paper, we will adopt this notational distinction between the two critical currents.

III. SAMPLES

Samples with three very different morphologies and two different chemical compositions were chosen for this study in order to provide considerable variation in characteristics which could be compared with the predictions of competing theoretical models.

The Ag/PBSCCO samples were made by an oxide/powder-in-tube method.[18] Oxide powders having a stoichiometry of $Bi_{1.8}Pb_{0.3}Sr_{1.9}Ca_{2.0}Cu_{3.1}O_{10}$ were produced by pyrolysis of nitrate solutions. The resulting powder was packed into silver tubes which were deformed by a combination of extrusion, drawing, and swaging into a hexagonal cross section. The wire was bundled and deformed again into a tape geometry. A final heat treatment formed a continuous multifilamentary matrix. The tapes prepared for the present study were cut from a length of tape produced during a pilot production run. The conductor had a cross section nominally 0.28 cm wide and 0.02 cm thick. Distributed throughout the Ag matrix were 19 superconducting filaments of PBSCCO (see inset to Fig. 1). Each filament consists of a layered array of grains. The total cross section of the tape was 5.6×10^{-3} cm^2; the cross section of the superconductor A_s was 23% of that value. The layered nature of the filaments raises the possibility that the superconducting properties might be anisotropic, in which case the AH model, which makes no provision for anisotropy, would appear to be inadequate. To characterize the anisotropy of this material we measured I_c when the magnetic field was oriented as shown in Fig. 1 and when it was rotated by 90 degrees. We found that at 4.2 K and when the magnetic field was varied from 0 to 20 T, the anisotropy was less than 7%.[19] Thus we apply the AH model with confidence.

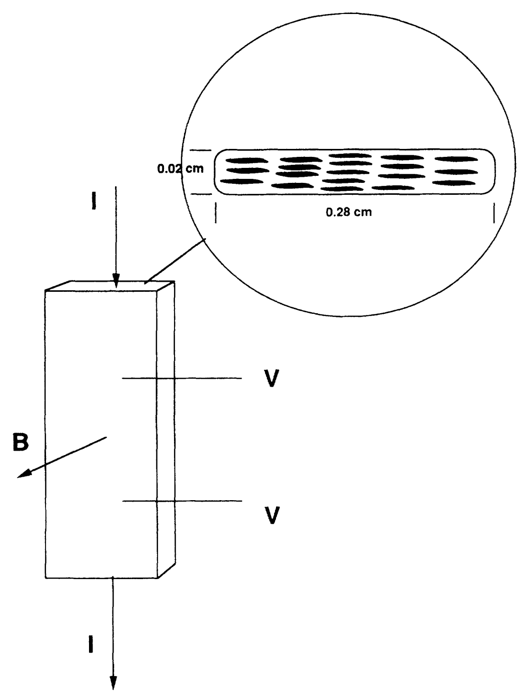

FIG. 1. Geometry of the composite $Ag/Bi_{1.8}Pb_{0.3}Sr_{1.9}Ca_{2.0}Cu_{3.1}O_{10}$ sample 3 showing the orientation of the applied current I and the applied magnetic field H. Inset: Cross section of the tape showing the 19 $Bi_{1.8}Pb_{0.3}Sr_{1.9}Ca_{2.0}Cu_{3.1}O_{10}$ filaments (black) imbedded in the Ag matrix (white).

Measurements were made on three short samples (4 cm long) which were numbered in chronological order as 1, 2, and 3. The last sample was studied the most extensively and is the one whose properties are reported here. The properties of the first two were taken over a more limited range of variables but, where there was overlap, they displayed behavior very similar to that of sample 3. Two much longer samples (each 30 m long), labeled 4 and 5, were wound into coils with an inner diameter of 2.92 cm, an outer diameter of 4.45 cm, and a length of 5.1 cm. Sample 5 was studied the most and will be reported here.

Figure 1 indicates for sample 3 the orientation of the applied current and magnetic field as well as location of the voltage and current leads. The voltage leads were soldered roughly 2 cm apart and 1 cm from the ends of the sample, whereas the current leads were soldered to each end. The resistance R of the sample was measured as a function of temperature in order to characterize the superconducting transition temperature T_c. $R(T)$ was found to be a linear function of temperature above 115 K, at which point it decreased rapidly until, at $T=109$ K, the resistance was zero. The midpoint of the transition occurred at $T_c=112$ K.

The YBCO films were deposited onto (100) $SrTiO_3$ substrates by a metalorganic deposition process.[20] The method consisted of spin coating a solution of barium, copper, and yttrium trifluoroacetates onto the substrate, followed by thermal decomposition to form an intermediate oxyfluoride material. The oxyfluoride was then heat treated in moist oxygen at high temperature to grow epitaxial YBCO. The films were 10–80 nm thick. A bridge 170 μm wide and 1.9 mm long was mechanically scribed into the film. T_c was measured to be 93 K.

The bulk YBCO samples were grown by a melt-texturing process in which the samples were grown from a liquid phase melt. They were relatively free of imperfections except for the presence of one or more grain boundaries purposefully grown in their interior.[21] The orientation and number of the grain boundaries could be carefully controlled by this growth process so that their effect on the I-V characteristic could be studied.

IV. EXPERIMENTAL PROCEDURES

The samples were mounted onto a cryostat which in turn was inserted into a double-walled dewar. The samples were immersed directly in the liquid cryogen filling the inner chamber of the dewar in order to promote isothermal conditions at all parts of the sample during the measurements. Three cryogens were used: liquid nitrogen, liquid neon, and liquid helium, so that the I-V curves were taken at the temperatures corresponding, respectively, to the normal boiling points at 77, 27, and 4.2 K. When liquid nitrogen and helium were used, the dewar was filled with the cryogen by transfer from a storage container and the gas boiloff was vented freely to the surrounding atmosphere. In the case of liquid neon, however, gas was condensed into the closed dewar space and the boiloff was recovered and stored in a leak-tight storage vessel for reuse.[22]

The dewar fit into the warm bore of two superconducting magnets. The first was a horizontal, superconducting Helmholtz coil, which could generate magnetic fields as large as 6 T. The second was a vertical, superconducting solenoid which could generate magnetic fields as large as 10 T. The short samples (Ag/PBSCCO, YBCO films, and melt-textured YBCO) were measured in the first magnet where the magnetic field was perpendicular to the current flow and perpendicular to the plane of the sample. The long samples of Ag/PBSCCO were measured in the second magnet where the magnetic field was perpendicular to the current but parallel to the plane of the sample.

I-V measurements were carried out using a computer for data acquisition and control. I-V curves were measured as the current was increased in programmed steps (typically in 0.1-A steps) and then decreased. A Keithley model 181 nanovoltmeter was used to measure the sample voltage, and a Keithley model 196 digital multimeter was used to measure the voltage at the current contacts. The current was supplied by a Hewlett Packard model 6032 system power supply.

V. RESULTS AND ANALYSIS

A. Ag/PBSCCO composite

The I-V curves for several values of magnetic field are shown for the Ag/PBSCCO composite sample 3 at three temperatures: $T=77$ K (Fig. 2), $T=27$ K (Fig. 3), and $T=4.2$ K (Fig. 4). The data points are shown by a variety of symbols, whereas the solid lines represent least-squares, four-parameter (I_c, γ, R_s, and G_n) fits of Eqs. (1) and (2) through the data. The parameter R_s is considered to be a macroscopic average value of the resistance of the PBSCCO material in the normal state, and thus differs from the quantity R_J defined by the AH model for a single junction. Generally the voltage ranged over four orders of magnitude from 0.1 μV to 1 mV: The lower limit was set by thermal emf drifts whereas the upper limit was set by the criterion that the sample was sufficiently far up the I-V curve to properly define G_n. The applied current varied from 0 to 50 A under these circumstances. Each curve includes data taken as the current was first increased and then decreased: There

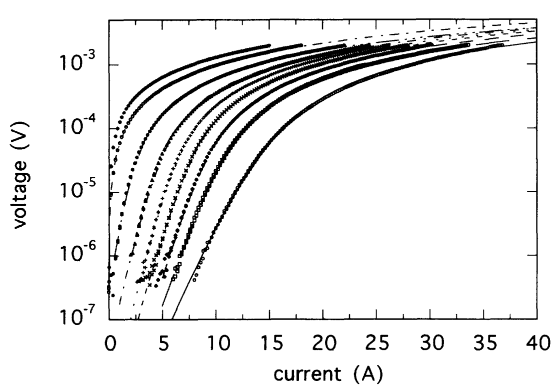

FIG. 2. Voltage-current characteristics of sample 3 at a temperature of 77 K as a function of applied magnetic field. Reading from upper left to lower right, the curves were taken at magnetic fields of 1.28, 0.64, 0.32, 0.16, 0.08, 0.04, 0.02, 0.01, and 0.0 T, respectively. The solid curves drawn through the data represent fits of the Ambegaokar-Halperin model.

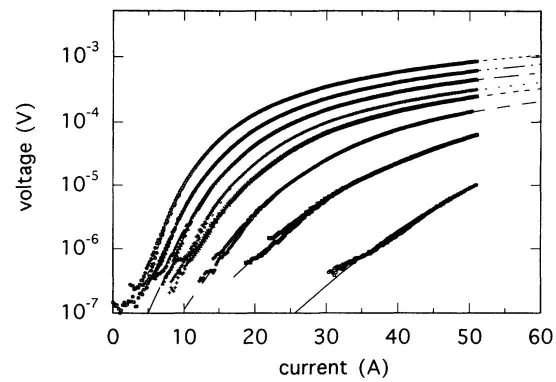

FIG. 3. Voltage-current characteristics of sample 3 at a temperature of 27 K as a function of applied magnetic field. Reading from upper left to lower right, the curves were taken at magnetic fields of 6.0, 4.0, 2.56, 1.28, 0.64, 0.16, 0.04, and 0.0 T, respectively. The solid curves drawn through the data represent fits of the Ambegaokar-Halperin model.

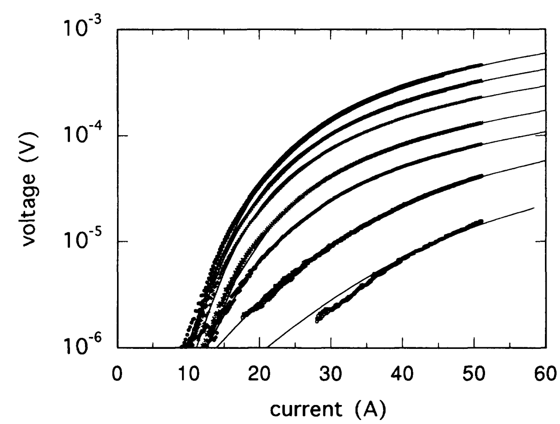

FIG. 4. Voltage-current characteristics of sample 3 at a temperature of 4.2 K as a function of applied magnetic field. Reading from upper left to lower right, the curves were taken at magnetic fields of 6.0, 4.0, 2.56, 1.28, 0.64, 0.16, and 0.04 T, respectively. The solid curves drawn through the data represent fits of the Ambegaokar-Halperin model.

was little or no evidence for hysteresis. The fit of the AH model to all of the data is very good. This being the case, values of G_n, R_s, I_c and γ obtained from the fits were well determined.

The fitting procedure was carried out as follows to take into account current sharing in the composite. First G_n was obtained by fitting the derivative $R_d = dV/dI$ obtained digitally from each *I-V* curve to Eq. (5). We found that more consistent values for G_n could be obtained by this procedure than by fitting the equation, $I = G_n V$ to the data for large I. Next I_s was obtained by the subtraction, $I_s = I - G_n V$; and then a least-squares fitting of the full integral equation (2) (which holds for values of γ and x) was carried out on the data set $V(I_s)$ to determine R_s, γ, and I_c.

The fitted values of the total resistance $R(H,T) = 1/G(H,T)$ are shown in Fig. 5(a). The total conductivity $G(H,T)$ of the composite is the parallel combination of the conductivities of the Ag and the PBSCCO, and is thus written $G = G_n + G_s = G_n + R_s^{-1}$. Since, however, $G_n \gg G_s$ (to be demonstrated shortly), the total conductivity should be nearly that of the silver. The magnetoresistance is clearly linear in H for $T = 27$ K and 4.2 K, with the same slope, although the linearity is less apparent at $T = 77$ K due to larger scatter. Such a linear dependence is expected for a polycrystalline Ag conductor[23] and thus supports the assumption that $G_n \gg G_s$. To further test this hypothesis, the resistance of a Ag tape, treated in the same way as the Ag/PBSCCO tape, was measured in a separate experiment. The temperature dependence of $R(0,T)$ obtained from this measurement was found to be within satisfactory agreement (10–20%) to the $H = 0$ intercepts $R(0,T)$ shown in Fig. 5(a).

The results for R_s are shown in Fig. 5(b). The scatter in the data is large (about 100%) due to the fact that the effect of this parameter on the fitting of the *I-V* curves was quite small. Nevertheless, it is clear that $R_s \gg R_n$ which supports the assertion used in the fitting procedure of the *I-V* curves. Furthermore, $R_s(H,T)$ has a much weaker percentage dependence on H than Ag in agreement with what has been observed in other high-temperature superconductors.[24]

The behavior of $I_c^{AH}(H,T)$ for the Ag/PBSCCO composite is shown in Fig. 6. The corresponding values for $J_c^{AH}(H,T)$, calculated by dividing I_c^{AH} by A_s, are shown on the right-hand axis. At all temperatures I_c^{AH} decreased rapidly as the magnetic field initially increased (i.e., when $H < 1$ T). Above 1 T, I_c^{AH} was almost constant at the two lower temperatures but it had all but vanished at 77 K. The figure also demonstrates that the magnitude of the critical current decreased strongly as the temperature was increased. These general features are similar to those observed for the critical current in granular YBCO and Tl-Ba-Ca-Cu-O.[25] Peterson and Ekin considered a granular superconductor as a network of strong superconducting material connected by a three-dimensional array of weakly coupled Josephson junctions. They predicted[26] that $J_c \sim H^{-3/2}$ for low magnetic fields where the Fraunhaufer diffraction patterns of $J_c(H,T)$ for each junction sum to this function. At higher magnetic fields the diffraction patterns of the Josephson junctions vanish and leave the more robust critical current of the bulk material which is comparatively independent of H. In Ref.

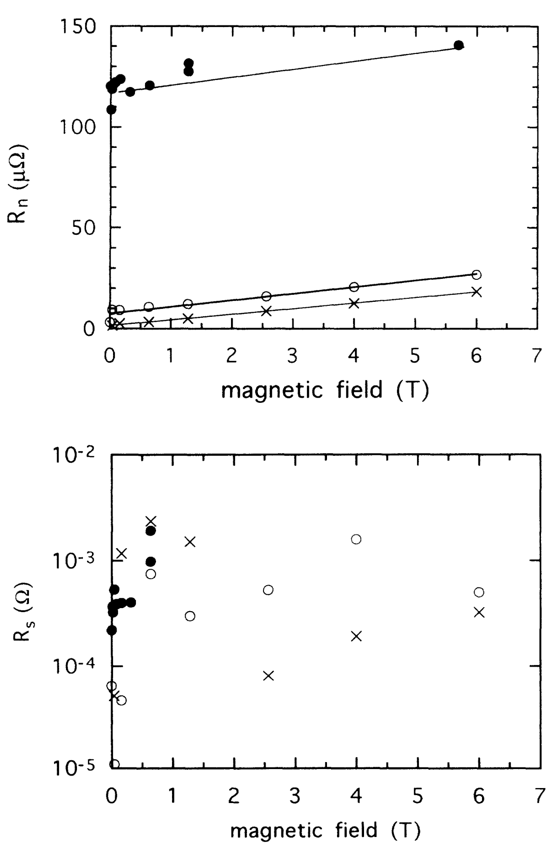

FIG. 5. (a) Magnetoresistance R_n of the Ag shunt at three temperatures: 77 K (●); 27 K (○); and 4.2 K (×). The solid lines represent least-squares linear fits through the data. (b) Magnetoresistance R_s of the $Bi_2Sr_2Ca_2Cu_3O$ in the normal state at three temperatures: 77 K (●); 27 K (○); and 4.2 K (×).

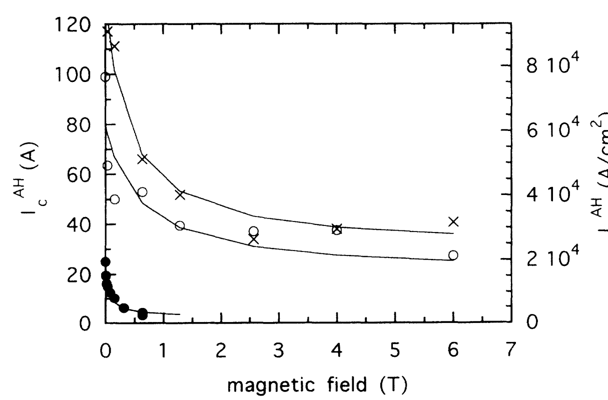

FIG. 6. Critical current I_c^{AH} (left-hand axis) and critical current density J_c^{AH} (right-hand axis) of sample 3 at three temperatures 77 K (●); 27 K (○); and 4.2 K (×) as a function of applied magnetic field. These quantities were obtained by fitting the measured *I-V* characteristics by the predictions of the Ambegaokar-Halperin model. The lines drawn through the data represent fits of Eq. (7).

25, the authors fitted their data at low magnetic fields to $J_c \sim H^{-m}$ and found that m varied between 1 to 1.5. We found the best representation of our data was a three-parameter equation:

$$I_c(H,T)=f(H,T)+g(T)\sim a(T)/[H+H_0(T)]+g(T) . \quad (7)$$

The parameter H_0 takes into account the presence of a field-independent intergranular pinning force in the spirit of the original model proposed by Anderson and Kim. The fitted values of H_0 were 0.05, 0.037, and 0.062 T at $T=4.2$, 27, and 77 K, respectively. From these results we judge that H_0 was independent of T and that its average value was comparable to that found for other superconductors (see Ref. 2). The function $g(T)$ represents the behavior of the critical current at high magnetic fields, and is therefore independent of H. We also found that the fitted values of $g(T)$ and $a(T)$ increased as the temperature decreased with functional forms proportional to $(1-t)^{3/2}$ which are consistent with predictions of the Ginsburg-Landau model. The solid curves shown in Fig. 6 represent fits of Eq. (7) to the data and the quality of the fits corroborates other evidence obtained from microscopy that the PBSCCO is indeed granular.

A comparison is made in Table I between the critical current defined by the Ambegaokar-Halperin model ($I_c^{\rm AH}$) and by a standard[27] 1 μV/cm criterion ($I_c^{\rm VC}$) obtained for sample 3 at a temperature of 27 K. The former exceeds the latter by a factor of between three to six. The dependence of $I_c^{\rm VC}$ on the magnetic field is similar to that shown for $I_c^{\rm AH}$ in Fig. 6.

The behavior of $\gamma(H,T)$ for the Ag/PBSCCO composite is shown in Fig. 7. The most striking feature is that γ was independent of magnetic field at 4 and 27 K, whereas it was strongly attenuated at 77 K when H was increased. When the data were fit by an equation identical in form to Eq. (7), we found that $g(T)$ was negligible at $T=77$ K, while at the lower temperatures $g(T)\sim$constant. Also clear from the figure is that $\gamma(0,T)$ has a value of 15–17, roughly independent of temperature. This implies through the definition, $\gamma=U(H,T)/k_BT$, that $U(0,T)\sim T$. The same temperature dependence has been inferred from data on grain-aligned powders of Y-Ba-Cu-O,[28,29] single crystals of Y-Ba-Cu-O,[30,31] irradiated Y-Ba-Cu-O crystals,[30] and Y-Ba-Cu-O thin films.[32] This behavior is not expected from the usual arguments about the pinning energy, however. That is, $U(H,T)$ is generally equated to the condensation energy for the superconducting state, in which case it is written as $[H_c^2(t)/8\pi]V_v$, where $H_c(t)=H_c(1-t^2)$ is the temperature-dependent critical magnetic field, V_v is the volume of the vortex, and $t=T/T_c$. V_v is the product of the cross-sectional area of the vortex ($\sim\pi r^2$) and its length (either ξ or a lattice spacing, d). The radius r of the vortex line is often set equal to ξ at low magnetic fields and to $(\phi_0/H)^{1/2}$ at high magnetic fields. Choice of the latter definition of r leads to the dependence $\gamma\sim H^{-1}$ which was observed at least at $T=77$ K for sample 3. Using the usual temperature dependence for ξ we conclude that $U(0,T)$ should approach a temperature-independent value as T approaches zero. Thus the temperature dependence expected from this line of reasoning contradicts that reported in this paper and in Refs. 28–32. If the postulate of a single pinning potential is replaced, however, by a distribution of potentials, then a linear temperature dependence is predicted.[33,34] Certainly for sample 3, this is a very reasonable assumption and is consistent with the granular nature of the material.

TABLE I. Comparison of the critical current defined by the Ambegaokar-Halperin model ($I_c^{\rm AH}$) and by a 1 μV/cm criterion ($I_c^{\rm VC}$) for a Ag/Bi-Sr-Ca-Cu-O composite (sample 3) at a temperature of 27 K.

H (T)	$I_c^{\rm AH}$ (A)	$I_c^{\rm VC}$ (A)
0.00	99.0	30.5
0.04	63.5	18.5
0.16	50.1	12.9
0.64	53.0	10.1
1.28	39.5	9.30
2.56	37.2	7.30
4.00	37.5	5.50
6.00	27.3	4.00

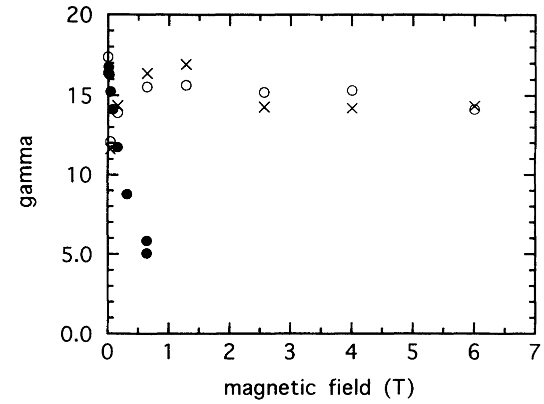

FIG. 7. γ of sample 3 at three temperatures 77 K (●); 27 K (○); and 4.2 K (×) as a function of applied magnetic field.

This completes the discussion of the behavior of the short Ag/PBSCCO samples typified by sample 3. Next the I-V characteristics of sample 5 were studied. Since this sample was 3000 times longer than sample 3 it thus offered an increase in sensitivity in electric field by the same factor for the same minimum voltage sensitivity. We found that the voltage noise of the coil increased, however, only netting a increase in range of E of 10. The results at $T=27$ K are shown in Fig. 8 as an example. The solid lines are fits of the AH model to the data and indicate that the model is remarkably successful. One possible conclusion to draw from the quality of these fits is that the 30 m length of sample 5 is as homogeneous as the 2 cm length measured in sample 3. This conclusion may be incorrect, however, because $V(I)$ predicted by the AH model is dominated by an exponential, and if the longer sample had a broader variation in $U(H,T)$, the largest value of $U(H,T)$ at each temperature would tend

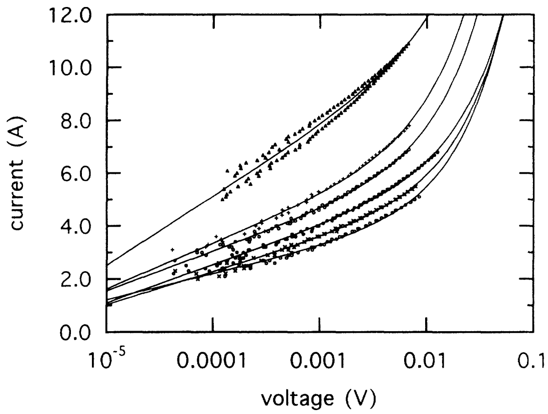

FIG. 8. *I-V* characteristics of sample 5 at a temperature of 27 K as a function of applied magnetic field. Reading from upper left to lower right, the curves were taken at magnetic fields of 0.0, 1.0, 2.0, 4.0, 6.0, and 8.0 T, respectively. The solid curves drawn through the data represent fits of the Ambegaokar-Halperin model.

to dominate the fits. Nevertheless, whatever the explanation for the success of the AH model, the fact that it fits a sample typical of that employed in a magnet represents cause for optimism that situations encountered in applications may be amenable to such modeling.

B. Other materials

All the discussion in this section thus far has been devoted to the observations and fitting of the *I-V* characteristics of the Ag/PBSCCO composite conductor. In order to test the applicability of the AH model to a wider range of circumstances, we incorporated other materials into the study.

Accordingly, short (1 cm), composite samples of Ag/PBSCCO prepared by a very different process (dynamic magnetic compaction) were studied as a function of magnetic field at $T = 77$ K. The resulting *I-V* curves were again fit well by the AH model.[35] Work is in pro-

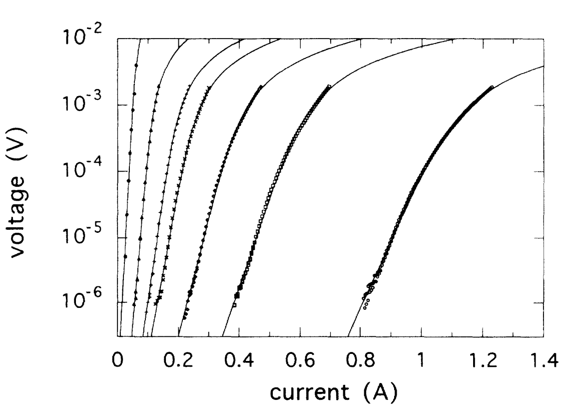

FIG. 9. Voltage-current characteristics of a Y-Ba-Cu-O thin film at a temperature of 77 K as a function of applied magnetic field. Reading from upper left to lower right, the curves were taken at magnetic fields of 3.0, 0.80, 0.30, 0.20, 0.10, 0.05, and 0.01 T, respectively. The solid curves drawn through the data represent fits of the Ambegaokar-Halperin model.

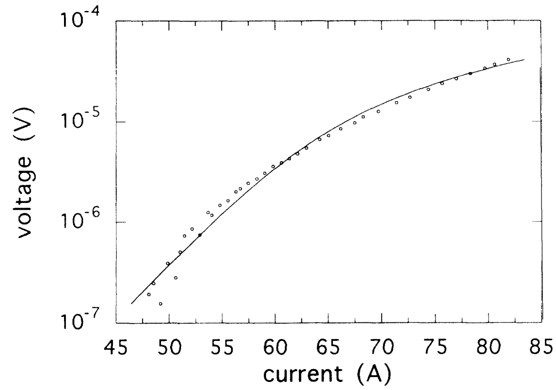

FIG. 10. Voltage-current characteristic of a melt-textured Y-Ba-Cu-O sample at a temperature of 77 K in 0.0 T. The solid curve drawn through the data represents a fit of the Ambegaokar-Halperin model.

gress to extend the study to other temperatures.

A more significant departure from these bulk PBSCCO studies was taken. The *I-V* curves of YBCO thin films have been characterized at 4 and 77 K; more extensive studies will be published elsewhere.[36] An example of the *I-V* curves and AH fits to them is shown in Fig. 9. These data were obtained at 77 K, while H ranged from 0.01 to 3.0 T. The fits by the AH model are excellent over the complete voltage range which extends down to 0.9 μV. Note that the current scale for the thin films is very different from the scale for the bulk PBSCCO.

Work has also begun on characterizing melt-textured, bulk YBCO. An example of an *I-V* curve taken at 77 K in zero magnetic field is shown in Fig. 10. A more complete study will be reported,[37] but the good fit of the AH model is apparent.

VI. ALTERNATIVE THEORIES

Several other theories have been advanced in order to characterize the dissipation of a superconductor in a magnetic field and consequently offer predictions for $I(V,H,T)$ which we also compared to our data.

In the *thermally activated flux-flow* (TAFF) model,[38] the physical picture differs from the Ambegaokar-Halperin model only in the choice of the pinning potential. In the AH model the potential is periodic, whereas in the TAFF model there is no stipulation that the pinning sites have any relation to each other. Individual flux lines or bundles of them hop from site to site. An attempt frequency for the process of lines hopping into and out of a pining site is calculated. The voltage is proportional to the attempt frequency and may be written as

$$V = V_0 \exp[-U(H,T)/k_B T] \sinh\{(J/J_c)\} \,, \tag{8a}$$

$$V = \sim V_0 \exp\{-\gamma(I - I_c)\} \,. \tag{8b}$$

Equation (8a) is similar to the AH prediction for small voltages [see Eq. (3)]. Equation (8b) is obtained for the condition that γ is large, as was the case for our experiments.

In the *collective flux-creep* (CFC) model,[11,12] and the *vortex-glass* (VG) model,[4] the vortex lines are not considered to be arranged in an orderly Abrikosov lattice. Instead they are presumed to assume a random, glasslike structure. The most compelling evidence which supports the latter model is based on the fact that the I-V curves may be scaled by functions of temperature so that all curves measured above a glass temperature, T_G, collapse to a common curve, while those measured at temperatures below T_G collapse to a different common curve. At T_G, which is generally close to T_c, the voltage is proportional to I^m, whereas below T_G it is given by the following equation:

$$V=V_0\exp\{\gamma[1-(I_c/I)^{\mu}]\}\ , \tag{9}$$

where μ is predicted to lie between 1 and 3. Note that for $\mu=1$ and $\gamma \gg 1$, the form of this equation is identical to the TAFF prediction. In this article, since we restricted measurements to the three temperatures provided by immersion in a liquid cryogen, we could not test the temperature scaling feature predicted by the VG model, but we could test the implication of Eq. (9).

Predating these theoretical efforts by many years and traditionally used to fit the I-V curves of low T_c materials is the *power-law* model. It has often been proposed on a purely empirical basis but it has also been derived from models which take into account sample imperfections such as a distribution of critical currents.[39] The power law is written as

$$V=V_0(I/I_c)^n\ . \tag{10}$$

This law is generally considered to apply to the very nonlinear region near $V\sim 0$ where the fitted values of n considerably exceed the limit at large voltages, where n must approach the value 1. This law has met with considerable success in fitting data for low T_c and high-T_c materials over a limited range of V.

All the equations above, except the one given by AH, have been written in forms such that $V=V_o$ when $J=J_c$. That is to say, J_c is defined in terms of a voltage criterion, which is defined by an arbitrary convention. By contrast, J_c is naturally incorporated into the AH model. An equation of the same form as Eq. (4) has been proposed by Gurevich *et al.*[40] on the basis of flux creep. That approach was sufficiently phenomenological, however, that the coefficients k_1 and k_2 could not be related to fundamental parameters. An advantage of the analysis presented here is that these coefficients are precisely defined by the AH model in terms of I_c, γ, and G.

The predictions of these models, embodied in Eqs. (8)–(10), were fitted to the same data already matched by the AH model [Eq. (2)]. The power law was moderately successful in fitting each I-V curve over a limited range of voltage but, as expected, was invariably unsuccessful in fitting the curves at large voltages where I became linear in V (i.e., where n must approach 1). Closer examination of Figs. 2–4, where $\ln V$ is plotted versus I, indicates clear deviations from linearity, thus eliminating the TAFF model by inspection. This leaves the vortex-glass model to contend with the AH model for the best explanation of the data. Generally we found that the VG fit the data moderately well over most experimental conditions but, in every case, the AH model fit even better. An example of the comparison of the fits of these two models to data taken at a temperature of 27 K and in a magnetic field of 0.16 T for sample 3 is shown in Fig. 11. The AH fits somewhat better (χ squared was a factor of 10 smaller) and also has the curvature which better matches the general shape of the data. Comparisons of this same nature and with the same conclusion were repeated for the data for 4, 27, and 77 K.

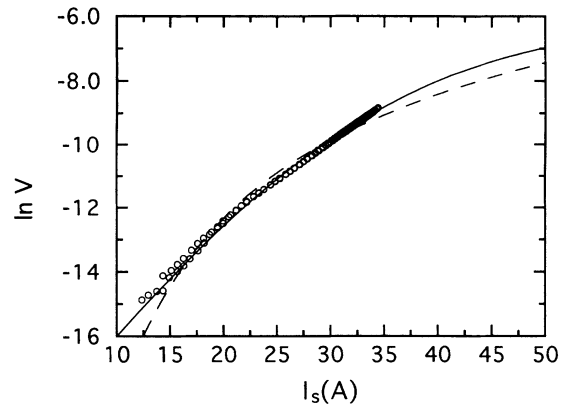

FIG. 11. Comparison of the fits of the vortex-glass (dashed line) and Ambegaokar-Halperin (solid line) models to the voltage-current characteristic (○) of sample 3 at $T=27$ K and $H=0.16$ T.

VII. CONCLUSION

We have measured the I-V characteristics of five composite Ag/PBSCCO samples, three of which were short and two of which were considerably longer. The I-V curves obtained as a function of magnetic field were extensively studied for a representative sample of each type. The measurements were carried out at three temperatures (4.2, 27, and 77 K). The results were fitted by equations predicted by four physical models (Ambegaokar-Halperin; flux creep; vortex glass; collective flux creep) and by an empirical one (power law). The fits strongly favored the Ambegaokar-Halperin model, from which the critical current $I_c^{\mathrm{AH}}(H,T)$ was obtained. To the knowledge of these authors this is the first time that this parameter has been defined for bulk superconductors purely on the basis of a physical law. Furthermore, the dependence of this parameter on temperature and magnetic field pointed to granularity of the PBSCCO as the principal cause of the dissipation. The pinning potential $U(H,T)$ also obtained from the fits may provide fundamental information which will prove useful for optimization of the critical current.

The predictions of other models were also fitted to the I-V curves reported in this study. The TAFF and power-law expressions were not as successful, but the VG equation provided fits to the curves which were almost as good as those provided by the AH model. In the case where two models fit almost equally well, consideration of additional factors may help to define the preferred choice. For instance, the plausibility of the temperature and magnetic-field dependence of γ and I_c obtained from fitting the AH model to the data may be compared to the behavior of μ and I_c obtained from the VG model. Unfortunately even these factors do not completely resolve this issue. For instance, the observation that $U(H,T) \sim T$ is argued in this paper as support for the AH model with a distribution of pinning potentials. The same phenomenon was used elsewhere to argue in favor of the VG model.[41]

Since the Ambegaokar-Halperin model was formulated for Josephson junctions, and since the PBSCCO part of this composite material consists of a network of individual grains for which the A-H model has shown to apply, it is perhaps not surprising that the model accounts so well for these observations. Nevertheless, analysis of the *I-V* characteristics of the Ag/PBSCCO composite was complicated by the fact that current sharing had to be taken into account. Since the conclusions reached in this article are based largely upon analysis of this material, their accuracy must wait for studies on other materials (noncomposites) such as those already launched for thin film YBCO (Ref. 20) and for melt-textured YBCO.[21] Clearly further study of the bulk-textured YBCO with the controlled insertion of a *single* grain boundary will do much to support the conclusions inferred from measurements of the multigrained PBSCCO. Conversely, studies of thin films and bulk materials without grains will test the wider applicability of the AH model. That the AH model appears to apply upon initial study with equal success to materials with other morphologies such as the thin films may point to the broader applicability of the AH model as suggested in Sec. II.

ACKNOWLEDGMENTS

The authors express their appreciation to M. Cima and K. Salama for permission to use their unpublished data. We are grateful to R. Buhrman, C. Lobb, and A. Malozemoff who clarified details of this article.

---

[1]T. T. M. Palstra, B. Batlogg, R. B. van Dover, L. F. Schneemeyer, and J. V. Waszczak, Phys. Rev. B **41**, 6621 (1990).

[2]P. W. Anderson and Y. B. Kim, Rev. Mod. Phys. **36**, 39 (1964).

[3]R. Koch, V. Foglietti, W. J. Gallagher, G. Koren, A. Gupta, and M. P. A. Fisher, Phys. Rev. Lett. **63**, 1511 (1989).

[4]Matthew P. A. Fisher, Phys. Rev. Lett. **62**, 1415 (1989).

[5]S. N. Coppersmith, M. Inui, and P. B. Littlewood, Phys. Rev. Lett. **64**, 2585 (1990).

[6]Vinay Ambegaokar and B. I. Halperin, Phys. Rev. Lett. **22**, 1364 (1969).

[7]R. Koch, V. Foglietti, and M. P. A. Fisher, Phys. Rev. Lett. **64**, 2586 (1990).

[8]A. C. Wright, K. Zhang, and A. Erbil, Phys. Rev. B **44**, 863 (1991).

[9]C. Gaffney, H. Peterson, and R. Bednar, Phys. Rev. B **48**, 3388 (1993).

[10]L. Miu, S. Popa, A. Crisan, G. Aldica, and J. Jaklovszky, J. Supercond. **6**, 279 (1993).

[11]M. V. Feigel'man, V. B. Geshkenbein, A. I. Larkin, and V. M. Vinokur, Phys. Rev. Lett. **63**, 2303 (1989).

[12]K. H. Fischer and T. Nattermann, Phys. Rev. B **43**, 10 372 (1991).

[13]See, for example, L. F. Goodrich and F. R. Fickett, Cryogenics **23**, 225 (1982).

[14]We found that Eq. (1) with I_s defined by Eq. (4) was a very good approximation to the correct *I-V* curve obtained by numerical integration (NI) of Eq. (2) for small values of $x = I/I_c$. In particular, we found that Eqs. (1) and (4) fitted the NI curve very well over several decades of x for $x < 0.3$ and that the fitted values of I_c, R, and γ agreed to within 5% of the values used in the numerical integration. For larger values of x, however, the fits became progressively worse and the fitted parameters deviated from the NI values by factors as large as 2.

[15]M. Tinkham and C. J. Lobb, *Solid State Physics: Advances in Research and Applications* (Academic, New York, 1989), Vol. 42, p. 91.

[16]M. Tinkham, Phys. Rev. Lett. **61**, 1658 (1988).

[17]R. J. Soulen, Jr., IEEE Trans. Appl. Supercond. **3**, 1261 (1993).

[18]M. J. Minot *et al.*, in *ICMC Conference Proceedings, Albequerque, NM, 1993* [Adv. Cryog. Eng. (to be published)].

[19]D. U. Gubser and T. Datta (private communication).

[20]P. C. McIntyre, M. J. Cima, and M. F. Ng, J. Appl. Phys. **68**, 4183 (1990).

[21]D. W. A. Willen and K. Salama, Physica C **201**, 311 (1992).

[22]T. L. Francavilla, R. J. Soulen, Jr., and J. H. Claassen, Rev. Sci. Instrum. **64**, 2023 (1993).

[23]Y. Iwasa, E. J. McNiff, R. H. Bellis, and K. Sato, Cryogenics **33**, 836 (1993).

[24]J. C. Ousset, S. Askenazy, H. Rakoto, J. M. Broto, J. F. Bobo, M. S. Osofsky, R. J. Soulen, Jr., and S. A. Wolf, in *High-T_c Superconductor Thin Films,* edited by L. Correra (Elsevier, New York, 1992), p. 25.

[25]J. W. Ekin, T. M. Larson, A. M. Hermann, Z. Z. Sheng, K. Togano, and H. Kumakura, Physica C **160**, 489 (1989).

[26]R. L. Peterson and J. W. Ekin, Phys. Rev. B **37**, 9848 (1988).

[27]In accordance with the prescription given in J. W. Ekin, Appl. Phys. Lett. **55**, 905 (1989), a line tangent to the *I-V* curve was drawn at the value $V = 1\ \mu$V. The intercept on the I axis defines the value I_c^{VC}.

[28]Y. Xu, M. Suenaga, A. R. Moodenbaugh, and D. G. Welch, Phys. Rev. B **40**, 10 882 (1989).

[29]I. A. Campbell, L. Fruchter, and R. Cabanel, Phys. Rev. Lett. **64**, 1561 (1990).

[30]C. Keller, H. H. Kuepfer, R. Meier-Hirmer, U. Weich, V. Selvamanickam, and K. Salama, Cryogenics **30**, 411 (1990).

[31]L. Civale, A. D. Marwick, M. W. McElfresh, T. K. Worthington, A. P. Malozemoff, F. Holtzberg, J. R. Thompson, and M. A. Kirk, Phys. Rev. Lett. **65**, 1164 (1990).

[32]G. M. Stollman, B. Dam, J. H. P. M. Emmen, and J. Pankert, Physica C **159**, 854 (1989).

[33]C. W. Hagen and R. Griessen, Phys. Rev. Lett. **62**, 2857 (1989).

[34]A. P. Malozemoff, T. K. Worthington, R. M. Yandrosky, and

Y. Yeshurun, Int. J. Mod. Phys. B **1**, 1293 (1988).

[35]T. L. Francavilla, R. J. Soulen, Jr., W. W. Fuller-Mora, P. Anderson, B. Chelluri, J. P. Barber, T. Scholtz, A. K. Sarkur, and D. H. Liebenberg, in *Processing of Long Lengths of Superconductors,* edited by U. Balachandran, E. W. Collings, and A. Goyal (The Minerals, Metals and Materials Society, Warrendale, PA, 1994), p. 253.

[36]P. C. McIntyre, M. J. Cima, D. H. Liebenberg, R. J. Soulen, Jr., T. L. Francavilla, and W. W. Fuller-Mora (unpublished).

[37]K. Salama, D. H. Liebenberg, R. J. Soulen, Jr., T. L. Francavilla, and W. W. Fuller-Mora (unpublished).

[38]P. W. Anderson, Phys. Rev. Lett. **9**, 309 (1962).

[39]W. H. Warnes and D. C. Larbalestier, Cryogenics **26**, 643 (1986); H. S. Edelman and D. C. Larbalestier, J. Appl. Phys. **74**, 3912 (1993).

[40]A. Gurevich, A. E. Pashitski, H. S. Edelman, and D. C. Larbalestier, Appl. Phys. Lett. **62**, 1688 (1993).

[41]A. P. Malozemoff and Matthew P. A. Fisher, Phys. Rev. B **42**, 6784 (1990).